Neuron
Article

Phosphorylation State of Olig2 Regulates Proliferation of Neural Progenitors

Yu Sun,[1] Dimphna H. Meijer,[1] John A. Alberta,[1] Shwetal Mehta,[1] Michael F. Kane,[1] An-Chi Tien,[2] Hui Fu,[1] Magdalena A. Petryniak,[2] Gregory B. Potter,[2] Zijing Liu,[1] James F. Powers,[3] I. Sophie Runquist,[1] David H. Rowitch,[2,*] and Charles D. Stiles[1,*]

[1]Department of Cancer Biology, Harvard Medical School and Dana-Farber Cancer Institute, 44 Binney Street, Boston, MA 02115, USA
[2]Departments of Pediatrics and Neurological Surgery, Howard Hughes Medical Institute, University of California, San Francisco, 513 Parnassus Avenue, San Francisco, CA 94143, USA
[3]Department of Pathology, Tufts Medical Center, Boston, MA 02111, USA
*Correspondence: rowitchd@peds.ucsf.edu (D.H.R.), charles_stiles@dfci.harvard.edu (C.D.S.)
DOI 10.1016/j.neuron.2011.02.005

SUMMARY

The bHLH transcription factors that regulate early development of the central nervous system can generally be classified as either antineural or proneural. Initial expression of antineural factors prevents cell cycle exit and thereby expands the pool of neural progenitors. Subsequent (and typically transient) expression of proneural factors promotes cell cycle exit, subtype specification, and differentiation. Against this backdrop, the bHLH transcription factor Olig2 in the oligodendrocyte lineage is unorthodox, showing antineural functions in multipotent CNS progenitor cells but also sustained expression and proneural functions in the formation of oligodendrocytes. We show here that the proliferative function of Olig2 is controlled by developmentally regulated phosphorylation of a conserved triple serine motif within the amino-terminal domain. In the phosphorylated state, Olig2 maintains antineural (i.e., promitotic) functions that are reflected in human glioma cells and in a genetically defined murine model of primary glioma.

INTRODUCTION

During central nervous system (CNS) development, regulation of pool size for diversified neuronal and glial progenitor populations involves complex interactions of spatially restricted organizing signals, mitogens, and other developmental cues that promote differentiation through intracellular signaling and activation of a variety of transcription factors (Edlund and Jessell, 1999). Proneural bHLH transcription factors (e.g., Ascl1) and antineurogenic bHLH and HLH transcription factors from the Hes, Hey, and Id families play pivotal roles in specification and differentiation of neurons and glia. At early times in development, antineurogenic factors prevail over their proneurogenic counterparts so as to sustain replication competence and expand the pool of neural progenitors. At later times, proneurogenic factors become dominant as to promote cell cycle exit, neuronal differentiation, and subtype specification (Jessell, 2000; Ross et al., 2003; Rowitch, 2004).

Oppositional functions of antineurogenic and proneurogenic transcription factors can be regulated at the level of gene expression or protein activity. In the developing telencephalon, for example, Delta/Notch signaling stimulates expression of antineural Hes transcription factors (reviewed in Justice and Jan, 2002), which in turn directly suppress expression of neural factor Ascl1. Conversely, suppression of Notch/Delta signaling (through relief of lateral inhibition) is needed for expression and function of proneural factors (reviewed in Beatus and Lendahl, 1998). According to the prevailing view of neurogenesis, the transient expression of proneural bHLH transcription factors such as Mash1, Ngn1, or Ngn2 induces a second sustained wave (or waves) of bHLH neuronal differentiation transcription factors (e.g., NeuroD, NeuroD2), which then promote terminal differentiation. Notably, neither proneural nor antineural bHLH transcription factors are generally expressed in fully formed, terminally differentiated neurons (Kageyama and Nakanishi, 1997; Lee, 1997). The proneural factor Ascl1 also plays a role in specification of oligodendrocytes (Parras et al., 2004). Even in this gliogenic context, however, Ascl1 expression is confined to immature precursors and is not seen in differentiated oligodendrocytes.

One neurogenic factor that defies this simple binary functional characterization is Olig2—a bHLH transcription factor that shows both antineural functions and proneural functions at different stages in the formation of the oligodendrocyte lineage. In the embryonic spinal cord, for example, Olig2 is expressed initially in the pMN domain, where it functions at early times in pattern formation (Lu et al., 2002) and as an antineural factor to sustain the replication competent state of those pMN progenitors that are destined for second wave gliogenesis (Lee et al., 2005) (see Discussion). Olig2 is likewise expressed in multipotent neurospheres derived from the embryonic forebrain, where it is required for optimum proliferation in vitro (Ligon et al., 2007). As development proceeds, Olig2 acquires a proneural function to specify formation of oligodendrocyte progenitors. However, unlike other proneural factors with roles in gliogenesis such as Ascl1 that are not expressed in their terminally differentiated end products (Parras et al., 2004), Olig2 expression is sustained

in oligodendrocyte progenitors and in mature oligodendrocytes (Lu et al., 2000), where it appears to have ongoing biological functions (Cai et al., 2007). A similar antineural/proneural dichotomy is observed in the postnatal brain, where Olig2 is expressed in rapidly cycling transit-amplifying cells ("Type C" cells) of the subventricular zone as well as in terminally differentiated myelinating oligodendrocytes that arise from these cells (Jackson et al., 2006; Menn et al., 2006).

Intuitively, it would seem that Olig2 cannot be doing the same thing in replication-competent progenitor cells and in terminally differentiated oligodendrocytes. The regulatory functions of Olig2 in proliferation of neural progenitors are of special interest due to provocative links to the literature on human gliomas. Tissue microarray and in situ hybridization studies show that Olig2 is expressed in 100% of the human diffuse gliomas, regardless of grade. Beyond merely marking the glioma cells, Olig2 expression is actually required for intracranial tumor formation in a murine model of glioma that recapitulates the genetics and histology of high-grade glioma in humans. The tumorigenic "gatekeeper" function of Olig2 reflects, at least in part, the fact that the gene encoding $p21^{WAF1/CIP1}$, a tumor suppressor and inhibitor of stem cell proliferation (hereafter referred to as "p21"), is directly repressed by Olig2 in murine neural progenitors and human gliomas (Ligon et al., 2007).

How might the distinct functions of Olig2 be dynamically modulated to suit biological context? Using mass spectroscopy, phosphorylation state-specific antibodies, and site-directed mutagenesis, we show here that the separate functions of Olig2 in progenitor self-renewal and oligodendrocyte development are controlled in part by developmentally regulated phosphorylation of a conserved triple serine motif within the amino-terminal domain. The promitotic functions of this triple serine motif are reflected in human glioma neurosphere cultures and in a murine model of primary glioma (the most common manifestation of the disease in humans) (Kleihues and Cavenee, 2007).

RESULTS

Identification of a Triple Phosphoserine Motif in Olig2

Using immunoaffinity chromatography, we purified microgram quantities of endogenous Olig2 protein from both normal murine neurosphere cultures and from gliomas generated by orthotopic transplant of primary human tumor neurospheres (see Figure S1 available online). High-confidence phosphorylation sites within Olig2 were mapped by mass spectroscopy (Figures 1, S1D, and S2). As indicated in Figure S1, a number of potential phosphorylation sites within Olig2 can be detected by computer algorithm. However, mass spectroscopy reveals that very few of these potential sites are actually utilized in endogenous Olig2 isolated from these murine and human progenitor cell types (see Discussion). Notably, no phosphorylated residues were detected within a serine/threonine-rich "box" that is a distinctive feature of all mammalian Olig2 homologs (Lu et al., 2000; Takebayashi et al., 2000; Zhou et al., 2000). Instead, high-confidence phosphorylation sites within endogenous Olig2 were confined to S10, S13, S14, and T43 within the amino-terminal domain (Figures 1A, S1, and S2).

The Triple Phosphoserine Motif in Olig2 Regulates Proliferation of Neural Progenitors in Secondary Neurosphere Assays

Olig2 null progenitor cells can be cultured as neurospheres in vitro. However, the population doubling time of *Olig2*-null progenitors is significantly extended relative to their wild-type counterparts (~43 versus ~35 hr, respectively) (Ligon et al., 2007). The four S/T residues comprising the high-confidence phosphorylation sites were mutated singly or in combinatorial fashion to glycine or valine so as to create phospho null Olig2 mutant proteins (Figure 1B). These phospho null variants were transduced into *Olig2*-null neural progenitor cells, and secondary neurosphere assays were conducted to examine their roles in proliferation.

As indicated (Figures 1C and 1D), the phosphorylation state of Olig2 is irrelevant to the total number of neurospheres that are produced in secondary neurosphere assays. However, the viable cell count within these neurospheres (and, hence, the size of the secondary neurospheres) is greatly reduced by phospho null substitutions at S10, S13, and S14 (triple phospho null [TPN]). Conversely, the substitution of negatively charged "phosphomimetic" amino acids (S -> D or S -> E) at this triple serine motif (triple phosphomimetic [TPM]) rescues the proliferative functions of wild-type Olig2 (Figures 1C, 1E, and 1F). The effects of these phospho null and phosphomimetic amino acid substitutions on proliferative functions of Olig2 were further confirmed by pulse-labeling experiments with BrdU (Figure S3).

Western blotting and immunostaining experiments show that the TPN and TPM substitutions affect neither the expression nor the subcellular location of Olig2; moreover, the total amount of ectopic wild-type or mutant Olig2 proteins (produced as transcription/translation products of our retroviral expression vectors) is roughly equivalent to the abundance of endogenous Olig2 protein in normal neural progenitor cells (Figure S4). Single or double substitutions at S10, 13, 14 proved to have minimal effect on neurosphere growth (Figure 1B). Accordingly, all of our further studies focused on the TPN and TPM variants shown in Figure 1B.

Phosphorylation State of the Olig2 S10/13/14 Motif Is Developmentally Regulated

Using synthetic phosphopeptides and affinity chromatography, we prepared a phosphorylation state-specific antibody to the Olig2 triple serine motif. Specificity of this antibody preparation was validated by western blot analysis of cells transduced with wild-type or phospho null variants of Olig2 (Figure 2A) and also by peptide competition western blots (Figure S6). Using this antibody, we examined the phosphorylation state of endogenous Olig2 in developing mouse embryos. Spinal cord is an anatomically simple region of the CNS, where the bifunctionality of Olig2 has been clearly documented. As indicated (Figure 2B), the phosphorylation state of Olig2 undergoes a dramatic decrease as proliferating Olig2-positive progenitors in the embryo mature into terminally differentiated, myelinating oligodendrocytes of the postnatal spinal cord. Developmental regulation of Olig2 phosphorylation can also be observed in vitro, when cycling progenitor cells are plated in factor-free medium and allowed to differentiate (Figure 2C). In cell culture it is possible to conduct pulse-labeling experiments with ^{32}P, and these experiments

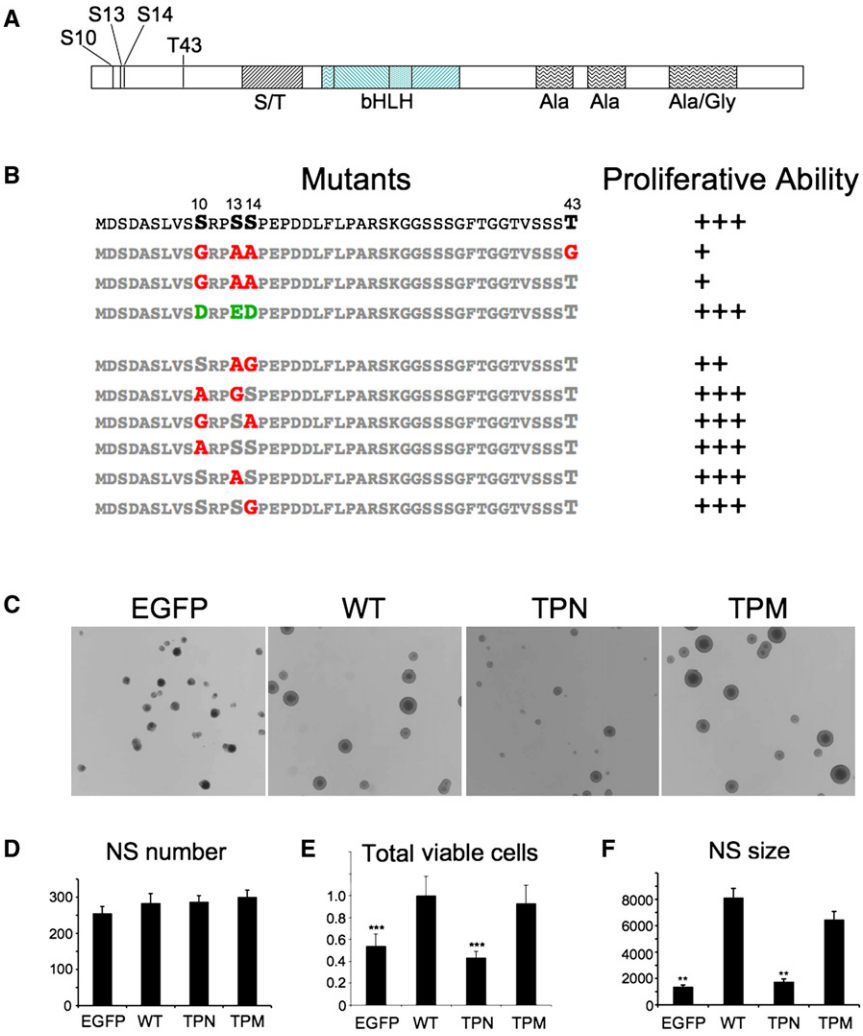

Figure 1. Triple Serine Phosphorylation Motif in the N Terminus of Olig2 Is Required for Proliferation of Neural Progenitor Cells

(A) Four phosphorylation sites were identified in the N terminus of Olig2 by mass spectroscopy. Three serine sites are in a tight cluster in the N terminus.

(B) We created a panel of single and multiple mutants of the phosphorylation sites. Olig2-null neural progenitor cells were transduced with each construct of Olig2 via retroviral infection. Secondary neurosphere assays were performed. Each construct was compared to Olig2 WT, and total viable cell population was used as an index for measuring neurosphere proliferative ability.

(C) Representative neurospheres generated from cells transduced with control vector (eGFP), Olig2 WT, Olig2 TPN, and Olig2 TPM reveal size differences.

(D) Secondary neurosphere numbers were compared. Transduced cells were plated in 6-well plates at 10 cells/μl (2 ml total volume) in EGF (20 ng/ml) and bFGF (20 ng/ml) containing medium. Seven days later, neurospheres from each well were counted using a dissection microscope. $p > 0.05$, one-way ANOVA. NS, neurosphere. Error bars, SEM.

(E) Total viable cell population was compared. One-way ANOVA and post hoc Newman-Keuls test, ***$p < 0.001$. Error bars, SD.

(F) Neurosphere sizes were measured with ImageJ software, and areas were compared. One-way ANOVA and post hoc Newman-Keuls test, **$p < 0.01$. NS, neurosphere. Error bars, SEM.

See also Figures S1–S3.

indicate that the developmentally regulated decline of phosphorylated Olig2 reflects diminished activity of an Olig2 protein kinase(s) (Figure 2D). Together these data indicate that the triple phosphorylation of Olig2 is correlated with proliferation of neural progenitor cells and is much diminished after differentiation.

Phosphorylation of Olig2 Is Dispensable for Specification and Terminal Differentiation of Oligodendrocytes

Targeted disruption of *Olig2* results in nearly complete ablation of the oligodendrocyte lineage in vivo and in vitro (Lu et al., 2002; Zhou and Anderson, 2002). As shown in Figures 3A and 3B, the ability of *Olig2*$^{-/-}$ progenitors to develop into O4-positive cells can be rescued by lentiviral transduction of wild-type *Olig2*; however, unlike the case with secondary neurosphere assays (Figure 1), the phospho null and phosphomimetic variants of Olig2 are equipotent to wild-type Olig2 for this developmental function (Figures 3C and 3D).

To determine whether phosphorylation of Olig2 is required for terminal differentiation of oligodendrocytes in vivo, we orthotopically transplanted *Olig2*$^{-/-}$ progenitors that had been transduced with vectors encoding either wild-type or phospho null Olig2 or GFP (control) into Shiverer (Shi) mice, which are null mutants for myelin basic protein (MBP). Because Shi mice produce no endogenous MBP, any detected MBP can be ascribed definitively to myelinating transplanted cells. As shown (Figures 4 and S5), wild-type and phospho null Olig2-transduced progenitors developed into oligodendrocytes with characteristic mature morphology and MBP production in vivo. We conclude that phosphorylation of Olig2 is dispensable for specification and terminal differentiation of oligodendrocyte lineage cells. These transplantation results do not rule out the possibility that phosphomimetic Olig2 might antagonize oligodendrocyte differentiation in vivo.

Phosphorylation State of the Olig2 Triple Serine Motif Correlates with Oncogenic Potential

Olig2 is expressed in 100% of the human diffuse gliomas regardless of grade (Ligon et al., 2004). Beyond merely marking malignant gliomas, Olig2 expression is required for intracranial tumor formation in a genetically relevant model of malignant glioma (Ligon et al., 2007). In this model, neural progenitor cells from *p16*^{Ink4a}/*p19*^{Arf} null mice are transduced with the mutated,

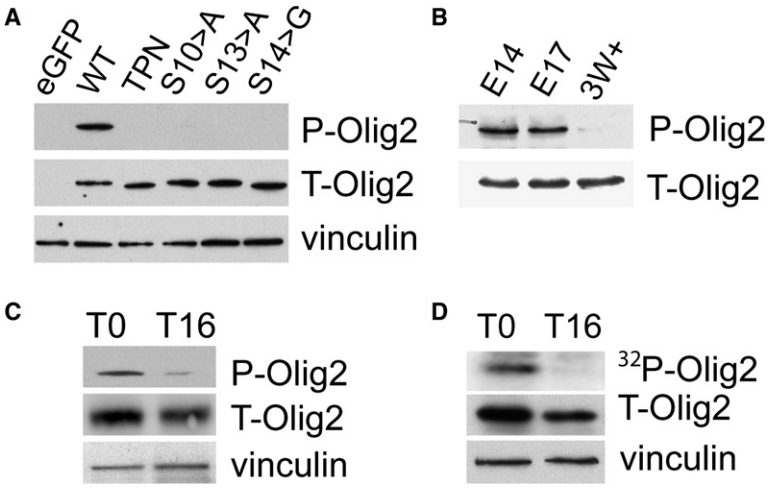

Figure 2. Triple Serine Phosphorylation State in Olig2 Is Regulated Developmentally

(A) Olig2 phospho-specific antibody detects phosphorylation in wild-type Olig2, but not in triple phosphomutant or any single serine mutant. Olig2-null neural progenitor cells bearing different Olig2 phosphorylation mutants were lysed, and the state of phosphorylation at S10, S13, and S14 was analyzed by western blot using phospho-specific Olig2 antibody. The blot was then stripped and reprobed with polyclonal antibody to total Olig2.

(B) Olig2 triple serine phosphorylation state decreases with increasing developmental stage of spinal cord. Whole spinal cords were dissected from E15 and E17 embryos and P23–25 CD1 mice. Protein lysates (40 μg) in RIPA buffer were loaded for immunoblotting, probed for phospho-Olig2 antibody, and then reprobed with a monoclonal Olig2 antibody.

(C) Triple serine phosphorylation decreased as neurospheres are allowed to become adherent and differentiate in growth factor-free medium. Olig2 WT neurospheres were rinsed once with ice-cold PBS medium and then plated in B27 containing medium in poly-l-ornithine coated plates. Sixteen hours later, cell lysates were collected and compared to undifferentiated neurosphere lysate (T0) by western blot.

(D) ^{32}P-pulse labeling of neurospheres in the presence (T0) or absence of EGF and bFGF. No ^{32}P incorporation in Olig2 is observed after overnight differentiation (16 hr). Autoradiogram (phosphorylated Olig2) and western blots (total Olig2 and vinculin loading control).

See also Figure S4.

constitutively active *EGFRvIII* variant of the epidermal growth factor receptor (Bachoo et al., 2002). These genetically engineered "tumor neurospheres" recapitulate two stereotypical genetic lesions that drive a high percentage of human gliomas (Kleihues and Cavenee, 2007; Cancer Genome Atlas Research Network, 2008).

As indicated in Figure 5, the malignant potential of *Olig2*-null tumor neurospheres is much impaired. Even when a high number ($\sim 10^5$) of *Olig*-null tumor neurospheres are inoculated into the brain, tumor penetrance is low, and latency is long. Tumor formation is rescued by transduction of wild-type Olig2 and the two Olig2 variants; however endpoint dilution experiments reveal a phosphorylation-dependent differential in the malignant phenotype. Relative to wild-type Olig2, both the lag time to tumor development and the minimum inoculum of tumor cells required for tumor formation are increased with the phospho null form of Olig2. Conversely, the phosphomimetic form of Olig2 is more tumorigenic than either wild-type or phospho null Olig2.

What about human gliomas? Although technically impractical to assess the function of Olig2 phosphorylation in the human tumors, we did use our phospho-specific antibody to interrogate Olig2 phosphorylation state within six human glioma neurosphere cultures. As reference points, we used Olig2 from cycling mouse neurosphere cultures and from terminally differentiated oligodendrocytes in the mouse corpus callosum. As indicated (Figure 6), the phosphorylation state of Olig2 was analogous to that of cycling murine progenitor cells rather than corpus callosum for five out of the six lines tested. Interestingly, the exception (one of six lines tested) was a *p53* null tumor cell line. In other studies we have found an intrinsic oppositional relationship between Olig2 and p53 (Mehta et al., 2011) such that Olig2 function (and presumably phosphorylation) is irrelevant in a p53 null context. Together, these findings indicate that Olig2 phosphorylation at the triple serine motif is present in human glioma and regulates tumor growth in a genetically relevant mouse orthotopic model.

Olig2 Phosphorylation State Regulates p53 Function

What is the molecular mechanism that links Olig2 phosphorylation to neurosphere growth and formation of malignant gliomas? A companion paper by Mehta et al. (2011) describes an intrinsic oppositional relationship between Olig2 and p53. Put briefly, Mehta et al. (2011) show that expression of Olig2 suppresses the posttranslational acetylation of p53, which is known to be required for optimum transcriptional functions (Barlev et al., 2001; Dornan et al., 2003). Concurrent with hypoacetylation, the interactions of p53 with promoter/enhancer elements of its stereotypical target genes (e.g., *p21*, *Bax*, *Mdm2*) are much attenuated in wild-type neural progenitors relative to their *Olig2*-null counterparts. Accordingly, p53-mediated biological responses to genotoxic damage are suppressed by Olig2.

Experiments summarized in Figure 7 show that this oppositional relationship between Olig2 and p53 is regulated by the phosphorylation state of the triple serine motif. Wild-type and also phosphomimetic Olig2 suppress the radiation-induced increase in both total p53 (Figure 7A) and acetylated p53 (Figure 7B). Likewise, wild-type and phosphomimetic Olig2 suppress radiation-induced expression of the canonical p53 target gene p21 (Figure 7C, inset). Concurrent with suppression of p21 expression, wild-type and phosphomimetic Olig2 promote the survival of irradiated neural progenitors, as noted by Mehta et al. (2011) (Figure 7C). In marked contrast, phospho null Olig2 is deficient in all of these functions.

In previous studies we have shown that basal levels of p21 expression seen in cycling neural progenitor cells are also suppressed by Olig2 (Ligon et al., 2007). As shown in Figure 8A (inset), wild-type and phosphomimetic Olig2 suppress basal levels of p21 protein, whereas phospho null Olig2 shows little

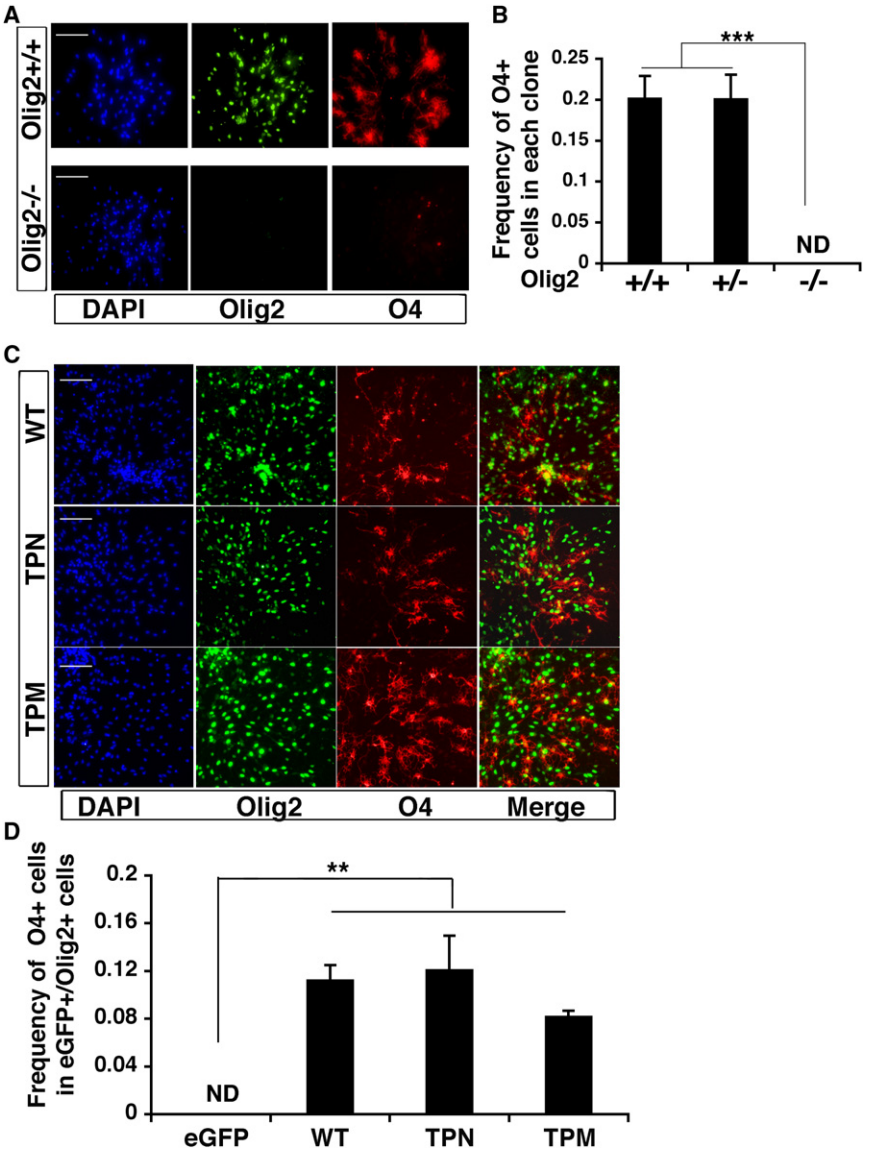

Figure 3. Triple Serine Phosphorylation in Olig2 Is Negligible in Specification of Oligodendrocytes

(A) Olig2 is required for the generation of O4-positive oligodendrocytes. Neural progenitor cells were isolated from the E12 LGE region, plated at clonal density, and cultured in bFGF-containing medium. Cells were stained with antibody to total Olig2 or O4 at day 7. Scale bar, 100 μm.

(B) The frequency of O4-positive cells was compared among *Olig2*$^{+/+}$, *Olig2*$^{+/-}$, and *Olig2*$^{-/-}$ embryos. ***p < 0.001, ANOVA and post hoc Newman-Keuls test; three embryos for each genotype. Error bars, SEM. ND, none detected.

(C) Triple serine phospho null, phosphomimetic, and Olig2 WT reveal similar abilities in rescuing O4-positive cells. Lentivirus bearing wild-type (WT), TPN, or TPM was used to infect Olig2-null E12 LGE progenitor cells at an MOI of 1:1. Cells were analyzed at day 9–10. Scale bar, 100 μm.

(D) The ratios of O4-positive cells among the infected cells (identified with either GFP or Olig2 staining) were compared. **p < 0.01, ANOVA and post hoc Newman-Keuls test (n = 3 independent experiments). ND, none detected. Error bars, SEM.

or no effect. The phospho Olig2-mediated suppression of p21 protein is exerted largely at transcriptional level, as indicated by diminished expression of *p21* mRNA (Figure 8A). Expression of a p21 luciferase reporter gene is likewise controlled by Olig2 in a phosphorylation state-dependent manner (Figure S8). This suppression of basal state *p21* mRNA reflects, at least in part, phospho Olig2-regulated changes in the amount of p53 that is associated with promoter/enhancer elements of the *p21* gene (Figure 8B). The differential loading of p53 onto p21 promoter enhancer element is nuanced but statistically significant and also in good accord with the basal state levels of acetylated p53 seen in Figure 7B.

On a final note, the phosphorylation state-dependent effects of Olig2 on neurosphere proliferation noted in Figure 1 are completely dependent on p53 status. As seen in Figures 8C and 8D, the phosphorylation state of Olig2 is irrelevant in p53 null neurospheres—at least with respect to cell proliferation. Collectively, these data show that p53 is a significant target of phosphorylated Olig2 in neural progenitors.

DISCUSSION

The bHLH transcription factor Olig2 is expressed in multipotent progenitors of the embryonic brain (Petryniak et al., 2007) and in the postnatal brain within cell types that span a biological continuum from rapidly cycling neural progenitors (e.g., type C cells, NG2 cells) to terminally differentiated, myelinating oligodendrocytes (Jackson et al., 2006; Ligon et al., 2006; Lu et al., 2000; Menn et al., 2006; Takebayashi et al., 2000; Zhou et al., 2000). How are the transcriptional functions of Olig2 modulated to suit these divergent biological contexts? We show here that a developmentally regulated phosphoserine motif in the amino terminus is essential for Olig2 proliferative function in both normal and malignant neural progenitors. On a mechanistic level the promitotic activity of this triple serine motif appears to reflect a suppression of p53 functions. In contrast to proliferative functions, specification and terminal differentiation of oligodendrocytes are completely independent of Olig2 triple serine phosphorylation state. In the fullness of time, the ability to uncouple proliferative and developmental functions of Olig2 may thus have practical applications in glioma medicine. In the interim the observations summarized here raise several interesting and unresolved scientific questions.

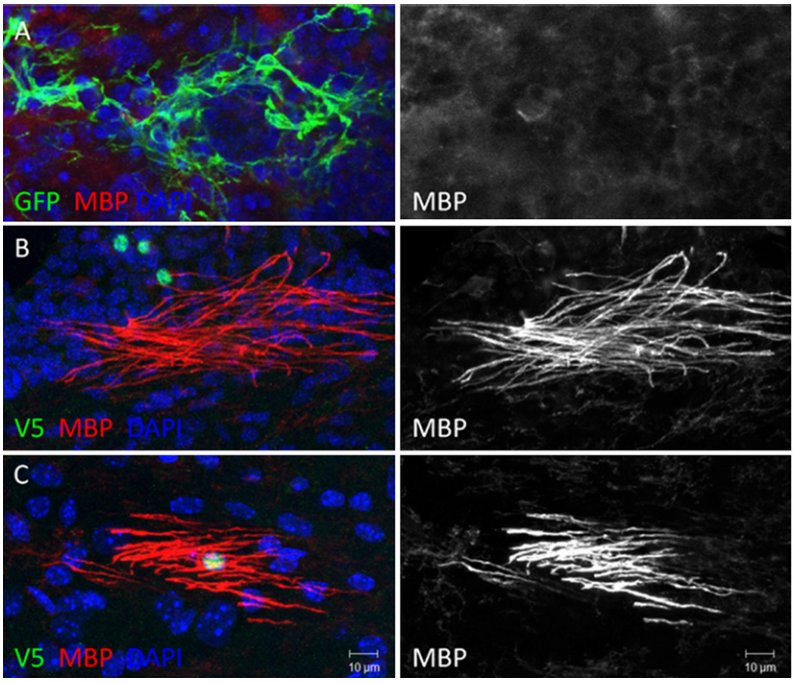

Figure 4. Triple Serine Phosphorylation in Olig2 Is Not Required for Maturation of Oligodendrocytes

Olig2-null neurospheres obtained from E14.5 *Olig2*$^{cre/cre}$ (null); *Rosa26-STOP-flox-eYFP* embryos were transduced with retrovirus containing expression constructs of eGFP, Olig2-V5 (WT), and Olig2-phospho null-V5 (TPN), respectively. Neurospheres were then transplanted into lateral ventricle of newborn Shi mice that lack MBP expression. The transplanted brains were sectioned and examined for MBP (red), eGFP (green in A), and V5 (green in B and C) expression. (A) Of the eGFP-positive Olig2-null cells, 0% expresses MBP, whereas 13.8% of the Olig2-V5 expressing cells and 16.4% of the Olig2-phospho null-V5 expressing cells express MBPs (B and C). See also Figure S5.

Are There Other Physiologically Relevant Phosphorylation Sites on Olig2?

Computer algorithms reveal a number of potential phosphorylation sites on Olig2 (Figure S1A). To determine which, if any, of these potential sites are actually utilized in neural stem cells, we developed a simple two-step protocol to purify microgram quantities of endogenous Olig2 from human glioma and murine neurosphere cultures. For comparative purposes we also purified ectopic Olig2 from COS cells transfected with a human Olig2 expression vector. Only a subset of the potential Olig2 phosphorylation sites cataloged is actually detected in these cells. Four amino acid residues, S10, S13, S14, and T43, scored as "high confidence" phosphorylation sites in all three of the cell types we examined.

It is possible that a small percentage of the Olig2 protein, below the detection limits of our mass spectroscopic analysis, is phosphorylated at other positions in biologically relevant cell contexts. This caveat must be considered in particular for potential phosphorylation motifs in the carboxyl terminal domain of Olig2, where proteolytic digestion sites are rather sparse. That said, we actually did detect a high-confidence phosphorylation site in the carboxyl terminus (S263) in ectopic Olig2 purified from transfected COS cells (data not shown). Another phosphoserine residue was found at S81 in the "S/T box" of COS cell-purified Olig2 (see below). However, we find no evidence that S81 or S263 is phosphorylated on the endogenous Olig2 protein expressed in neural cell types. As previously reported, a considerable fraction of ectopic Olig2 in transfected COS cells is mislocalized to the cytosol (Sun et al., 2003). The level of ectopic Olig2 generated by COS cell expression vectors is so high that we did not need to use isolated nuclei as a source of starting material for our protein preparations and, instead, extracted both nuclear and cytosolic Olig2. For these reasons we are inclined to regard the S81 and S263 phosphorylation events as cytosol-specific artifacts of the COS cell system.

Setoguchi and Kondo (2004) have suggested (on the basis of in vitro phosphorylation studies) that AKT-mediated phosphorylation of S30 causes Olig2 to relocalize from the nucleus to the cytosol, where it is subsequently degraded to allow formation of astrocytes from neural progenitor cells. We did not detect any evidence of S30 phosphorylation in nuclear extracts of the neural cell types we studied. However, S30 was detected as a low-confidence phosphorylation site in COS cell extracts. The detection of low levels of phospho S30 in our mass spectroscopy analysis of COS cell Olig2 may have been enabled by the large amounts of cytosolic Olig2 in the COS cell preparations and would thus be consistent with a degradative role of S30, as suggested by Setoguchi and Kondo (2004) (but see below).

Phylogenetic Conservation of the Triple Serine Motif in Vertebrates

Critical primary and secondary structural features of proteins are conserved through evolution. Myelinating oligodendrocytes are detected in all vertebrates above the jawless fish. As indicated in Figure S7, the triple serine motif and its flanking amino acid residues are well conserved in Olig2 from human down through zebrafish. In fact, the triple serine motif of Olig2 is nearly as well conserved as the DNA-targeting bHLH motif. The other high-confidence phosphorylation site at T43 is likewise well conserved. By contrast the S30 region of Olig2 (Setoguchi and Kondo, 2004) does not seem to be well conserved.

Murine Olig2 and its close structural homolog Olig1 contain a serine/threonine-rich "box" toward the amino-terminal side of the DNA-targeting bHLH domain (Lu et al., 2000; Takebayashi et al., 2000; Zhou et al., 2000). In murine Olig2 this S/T box is an especially distinctive feature, containing 11 contiguous S or T residues beginning at S77 and ending at S88 (Figure S1). We were somewhat surprised that our mass spectroscopy analysis of endogenous Olig2 detected no evidence of phosphoserine or phosphothreonine residues within this S/T box.

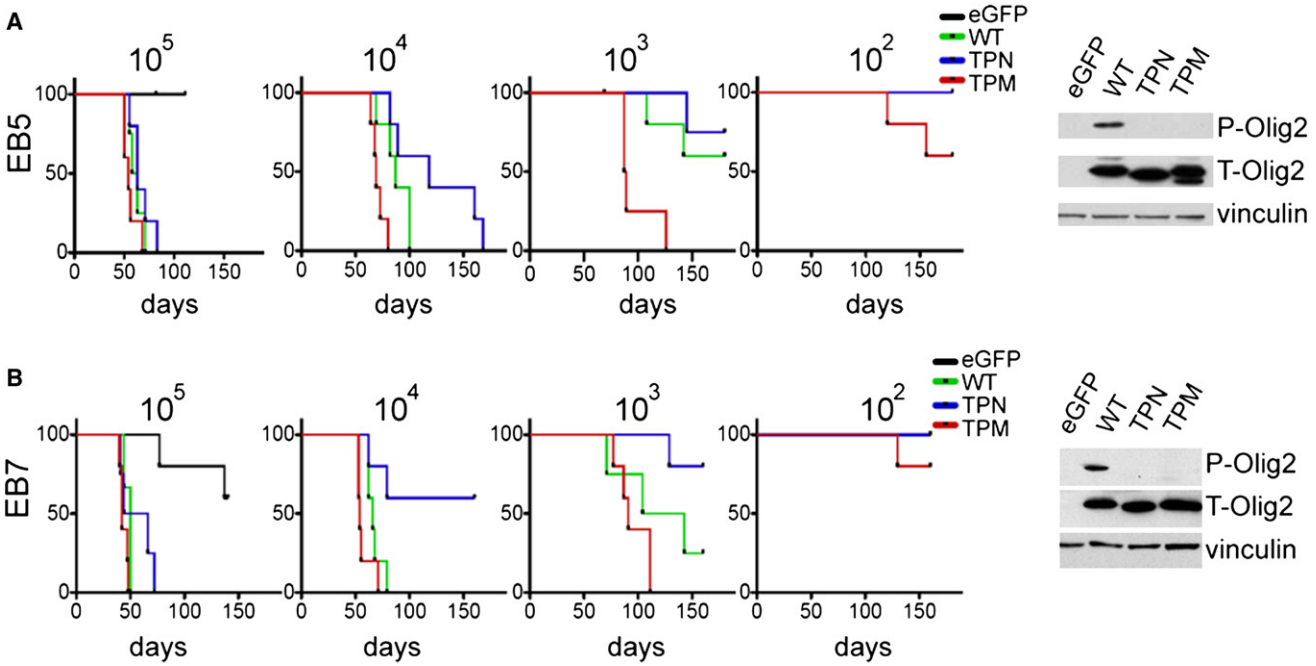

Figure 5. Phosphorylation State of the Olig2 Triple Serine Motif Correlates with Oncogenic Potential

(A) *Ink4a*$^{-/-}$*Arf*$^{-/-}$ *Olig2*$^{-/-}$ *EGFRVIII* murine neural progenitor cell line EB5 was stably transduced with eGFP, Olig2 WT, Olig2 triple null (TPN), or Olig2 phosphomimetic (TPM) via retroviral infection. Tumorigenic potential of each line was compared using a limiting dilution assay. For each construct, 10^5, 10^4, 10^3, or 10^2 dissociated neural progenitor cells were injected intracranially, and the survival of each mouse was recorded (for the eGFP control group, 10^5 were injected). Expression levels of each Olig2 construct in the EB5 line were examined by western blot for phosphorylated Olig2 and total Olig2 (right panel). Vinculin expression was used as a loading control.

(B) Same as (A) but with another independently derived *Ink4a*$^{-/-}$*Arf*$^{-/-}$ *Olig2*$^{-/-}$ *EGFRVIII* murine neural progenitor cell line, EB7.

DNA sequence analysis reveals that the S/T box diverges rapidly down through phylogeny (in contrast to the triple serine motif). Beginning with chicken and moving downward to *Xenopus* Olig2, an increasing number of the serines are replaced by alanine residues. In space-filling models, alanine and serine residues are roughly equivalent, suggesting that size rather than phosphorylation potential is the critical structural feature of the S/T box. However, at the level of zebrafish, even this small-volume "S/T" box has largely disappeared. In addition it should be noted that no version of vertebrate Olig3 displays an S/T box, even though mammalian Olig3 proteins are virtually identical to mammalian Olig2 within the DNA-targeting bHLH motif (Takebayashi et al., 2000).

Developmental Regulation of Replication Competence by Olig2 in the CNS

In this study we have focused on evolving functions of Olig2 in multipotent progenitors of the developing forebrain and in myelinating oligodendrocytes of the postnatal brain. However, in the developing spinal cord, Olig2 is expressed initially in the pMN domain, where it functions at early times to sustain the replication competent state of those pMN progenitors that give rise to oligodendrocytes (Lee et al., 2005). Olig2 function is also required for neural patterning and specification of motor neurons and oligodendrocyte progenitors (Lu et al., 2002; Novitch et al., 2001; Park et al., 2002; Takebayashi et al., 2002; Zhou and Anderson, 2002). So, might phosphorylation of the Olig2 triple serine motif also be responsible for the developmental switch from pMN progenitor proliferation to cell fate specification in the embryo? The answer to this question may be complex. Indeed, *Olig2*-null animals show no obvious proliferation phenotype in spinal cord or brain (Lu et al., 2002; Novitch et al., 2001; Park et al., 2002; Takebayashi et al., 2002; Zhou and Anderson, 2002). This lack of a proliferation phenotype is most probably accounted for by the dramatic changes in neural patterning in *Olig2*-null embryos, whereby the pMN domain is respecified to p2 fate, coupled with the fact that the p2 domain contains independent mechanisms for cell cycle regulation capable of supporting similar levels of progenitor proliferation. Therefore, further work using knockin mutants of phospho null *Olig2* is required to investigate possible roles for Olig2 in embryonic progenitor proliferation, and such studies are in progress.

Regulation of p53 Functions by the Triple Serine Motif

In a companion paper, Mehta et al. (2011) show that Olig2 suppresses radiation-induced functions of p53 in both normal and malignant neural progenitors. We show here that this intrinsic oppositional relationship between Olig2 and p53 is regulated by the Olig2 triple serine motif. Wild-type and also phosphomimetic Olig2 suppress the classic radiation-induced accumulation of p53 protein, whereas phospho null Olig2 is permissive for this response (Figure 7A). We have generated mRNA expression profiles on Olig2 wild-type, Olig2-null, Olig2 phospho null, and Olig2 phosphomimetic neurospheres. These

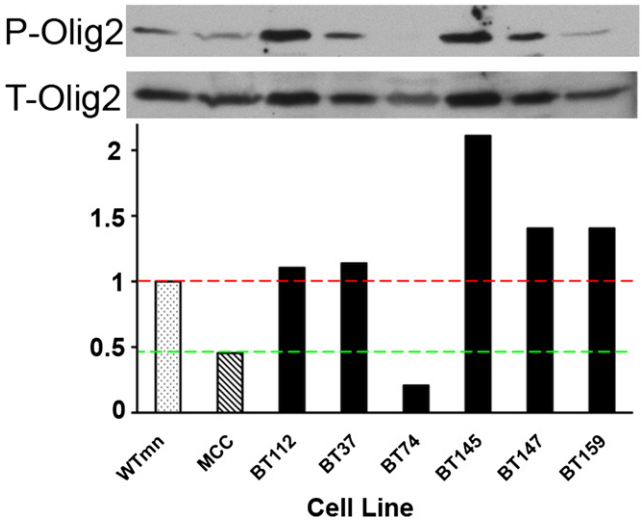

Figure 6. Phosphorylation of Olig2 in Human Glioma Cell Lines
Several human glioma cell lines were examined for their levels of Olig2 phosphorylation using the phosphorylation state-specific antibody by western blot. WTmn, wild-type mouse neurospheres; MCC, mouse corpus callosum; BT, brain tumor cell line. Western blots were quantitated using a Typhoon Imaging System, and values in the graph are representative of three independent repeats. BT74 denotes the only human tumor cell line in this study that harbors a mutant form of p53. See also Figure S6.

profiles reveal no impact of Olig2 proteins on the level of p53 mRNA levels (data not shown). Rather, it appears that wild-type and phosphomimetic Olig2 suppress radiation-induced posttranslational acetylation events that enhance both the stability (Li et al., 2002) and the transcriptional functions (Barlev et al., 2001) of p53 (Figure 7B).

In addition to their guardian functions in response to genotoxic damage, p53 and p21 are known to regulate the proliferation of normal neural progenitors (Kippin et al., 2005; Meletis et al., 2006). As shown in Figure 8, wild-type and phosphomimetic Olig2 suppress basal expression of p21 protein and mRNA in cycling cells. These effects are reflected, at least in part, by diminished levels of p53 protein associated with promoter/enhancer elements of the *p21* gene. However, the pronounced impact of Olig2 phosphorylation on expression of p21 protein and mRNA (Figure 8A) stands somewhat in contrast to the more nuanced differences in total p53 bound to *p21* promoter/enhancer elements (Figure 8B). Expression of p21 protein and mRNA is likely to reflect the cumulative impact of reduced p53 recruitment to the p21 promoter, reduced transcriptional function of hypoacetylated p53 at the promoter (Barlev et al., 2001), and possible posttranscriptional effects on stability of the p21 protein (Coleman et al., 2003; Gong et al., 2003). In addition we have shown in previous studies that Olig2 can interact directly with the promoter/enhancer elements of *p21* (Ligon et al., 2007). Because Olig2 has been characterized as a transcription repressor (Novitch et al., 2001; Zhou et al., 2001), it is possible that the attenuation of p53 transcriptional functions is further augmented by direct Olig2-mediated suppression of *p21* expression (however, see below). Notwithstanding the complexity of p21 regulatory mechanisms, the experiment summarized in Figures 8C and 8D shows clearly that p53 is a prime target of the Olig2 proliferative phenotype.

Regulation of Olig2 Functions by the Triple Serine Motif

How does phosphorylation of the triple serine motif affect transcriptional functions of Olig2? Members of the bHLH transcription factor family function as homodimers or as heterodimers with E12/E47 proteins to bind to canonical E box elements in the promoter/enhancer regions of their target genes (Ross et al., 2003). The bHLH motif is almost exclusively responsible for both heterodimerization and DNA targeting to the E box. It seems unlikely that phosphorylation events in the amino terminus would have any direct effect on these functions of Olig2, and preliminary chromatin immunoprecipitation (ChIP) studies failed to show changes in Olig2:p21 targeting that could account for the effects on basal p21 expression of p21 seen in Figure 8A.

The fact that all three serine residues at positions 10, 13, and 14 must be mutated to achieve a strong loss-of-function or gain-of-function phenotype suggests that the proliferative function associated with the Olig2 phosphorylation state involves a significant conformational change in the amino terminus of Olig2. This conformational change could affect the interaction of Olig2 with DNA or important coregulator proteins and, thus, affect the transcriptional activity of Olig2 upon target genes that affect p53 function. One final possibility that cannot be ruled out by the data is that the p53 antagonist function of Olig2 is independent of its function as a bHLH transcription factor. It is possible, for example, that phosphorylated Olig2 competes directly with p53 for binding to proteins that promote p53 acetylation or prevent its deacetylation. In fact preliminary observations of Mehta et al. (2011) suggest such a mechanism.

Phosphorylation State of Olig2 and Malignant Potential

In a murine model of primary glioma, the tumor penetrance is quite low, and latency is prolonged in the absence of Olig2 expression (Figure 5; Ligon et al. [2007]). A forced phosphomimetic Olig2 state actually enhances intracranial tumor formation relative to wild-type Olig2. We speculate that the enhanced performance of the phosphomimetic Olig2 relative to the wild-type protein in vivo reflects the fact that some of the implanted cells expressing wild-type Olig2 undergo differentiation with attendant dephosphorylation, whereas the mutant form of Olig2 is locked into a phosphomimetic configuration.

An unexplained feature of the limiting dilution assays for tumor growth (Figure 5) is that the phospho null form of Olig2, though clearly inferior to wild-type and phosphomimetic Olig2, is able to support tumor growth when large numbers of cells are transplanted. Based on the p21 suppression results, particularly the inability of the TPN mutant form of Olig2 to suppress p21, one might predict that phospho null Olig2 would be completely nontumorigenic. How does one account for the residual tumorigenic potential of phospho null Olig2? In a companion paper to this one, Mehta et al. (2011) show that the major role of Olig2 in promoting intracranial tumor formation is to suppress the functions of p53. However, these workers also noted a somewhat nuanced p53-independent function(s) of Olig2 in tumor formation. It is possible that the p53-independent functions of Olig2

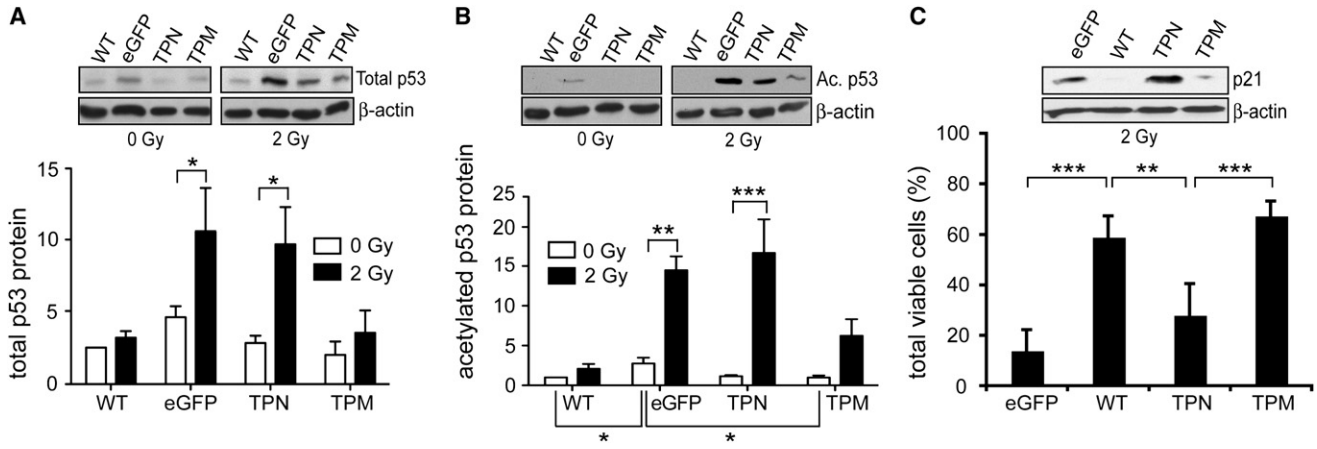

Figure 7. Wild-Type and Phosphomimetic Olig2 Suppress Radiation-Induced p53 Responses

(A) Phosphorylation state of Olig2 affects DNA damage-induced accumulation of p53 protein. *Olig2*$^{-/-}$ mouse neural progenitor cells were stably transduced with a vector control (eGFP) or with Olig2 WT, Olig2 TPN, or TPM as indicated. Cells were either untreated or treated with 2 Gy of IR, and lysates were obtained in presence of HDAC inhibitor, size fractionated, and immunoblotted with antibodies recognizing p53 or β-actin. The experiments were repeated a total of five times. The resulting immunoblots (inset) were normalized for β-actin and quantified (bar graphs). As indicated, wild-type and also phosphomimetic Olig2 suppress radiation-induced changes in total p53, but phospho null Olig2 is without effect (*$p < 0.01$, two-way ANOVA and Bonferroni post hoc test). In nonirradiated cells (white bars), the differences in total p53 between the four experimental groups did not approach the level of statistical significance. Error bars, SEM.

(B) Phosphorylation state of Olig2 affects DNA damage-induced acetylation of p53 protein. Same as (A), except that cell lysates immunoblotted with antibodies recognize acetylated p53 (Lys379) or β-actin. Again, wild-type and phosphomimetic Olig2 suppress radiation-induced changes in acetylated p53, whereas phospho null Olig2 is without effect (*$p < 0.05$). Relative to vector controls, wild-type and phosphomimetic Olig2 create a small, but significant, suppression of acetylated p53 in nonirradiated cells (white bars). *$p < 0.05$, **$p < 0.01$, ***$p < 0.001$, two-way ANOVA and Bonferroni post hoc test. Error bars, SEM.

(C) Inset shows that phosphorylation state of Olig2 dictates p21 expression level and cell survival following gamma irradiation. Cells were irradiated with 2 Gy IR. Endogenous p21 expression levels were compared by western blot with β-actin as a loading control. Bar graph shows relative cell growth after 2 Gy irradiation. Total viable cells are defined as the percentage of viable cells 4–5 days after treatment compared to nontreatment groups. Data presented are from three independent experiments. Error bar, SD. One-way ANOVA, $p < 0.001$. Post hoc Newman-Keuls test, **$p < 0.01$ and ***$p < 0.001$.

in tumor formation noted by Mehta et al. (2011) are likewise independent of phosphorylation state.

The Triple Serine Motif as a Drug Target for Malignant Glioma

Chemical tool compounds and hairpin RNA expression vectors, used in combination with our phospho-specific antibody (Figure 2), should ultimately lead to identification of protein kinases that regulate the phosphorylation state of S10, S13, and S14. Phosphorylation modeling programs such as Scansite, GPS, and PredPhospho as well as direct evaluation yield some overlapping predictions for kinase candidates but also different predictions for each of the three serine residues. Among the best-represented predictions are CDK5, ERK kinases (ERK1, 2/MAPK), GSK3, and casein kinases (CK1/2). In neurosphere proliferation assays we were unable to narrow the phenotype of TPN Olig2 down to a single serine site, which argues against the existence of a priming site. However, an intramolecular cascade may be operative if GSK3 acts at Ser10, as predicted by the computer algorithms. GSK3 would require prephosphorylation of Ser14 to create the motif S/TXXXpS/pT. Likewise, phosphorylation of Ser13 is prerequisite for CK2 to phosphorylate S10 (PhosphoMotif, http://www.hprd.org).

Olig2 is a lineage-restricted regulatory transcription factor whose expression is confined to the CNS. The expression pattern of Olig2 in human tissue microarrays (Ligon et al., 2004), combined with mouse modeling studies of human glioma (Ligon et al., 2007), has suggested to us that a small molecule inhibitor of Olig2 might serve as a targeted therapeutic for a wide range of pediatric and adult gliomas. However, an antitumor therapy that generally targets all Olig2 activity in the brain (e.g., by shRNA) would likely have detrimental, off-target effects in nontumor cells, such as oligodendrocytes potentially limiting tolerance/utility. Moreover, transcription factors are generally considered unattractive targets for drug development because their interactions with DNA and with coregulator proteins involve large and complex surface area contacts.

In contrast to transcription factors, protein kinases lend themselves readily to the development of potent and specific small molecule inhibitors. Our studies indicate that Olig2 functions critical for glioma growth (Figure 5) and radiation resistance (Figure 7), but not development (Figures 3 and 4), are distinguished by the triple serine phosphorylation. The ability to uncouple these functions one from the other suggests an avenue to specifically target Olig2-dependent tumors within the brain while sparing normal white matter. In the fullness of time, small molecule inhibitors of Olig2 protein kinases could have practical overtones for patients with glioma and provide a more specific means of therapy with minimized off-target effects in oligodendrocytes.

EXPERIMENTAL PROCEDURES

Animal Procedures, Tissue Dissociation, and Cell Culture

Animal husbandry was performed according to DFCI and UCSF guidelines under IACUC-approved protocols for all experiments reported. The strains

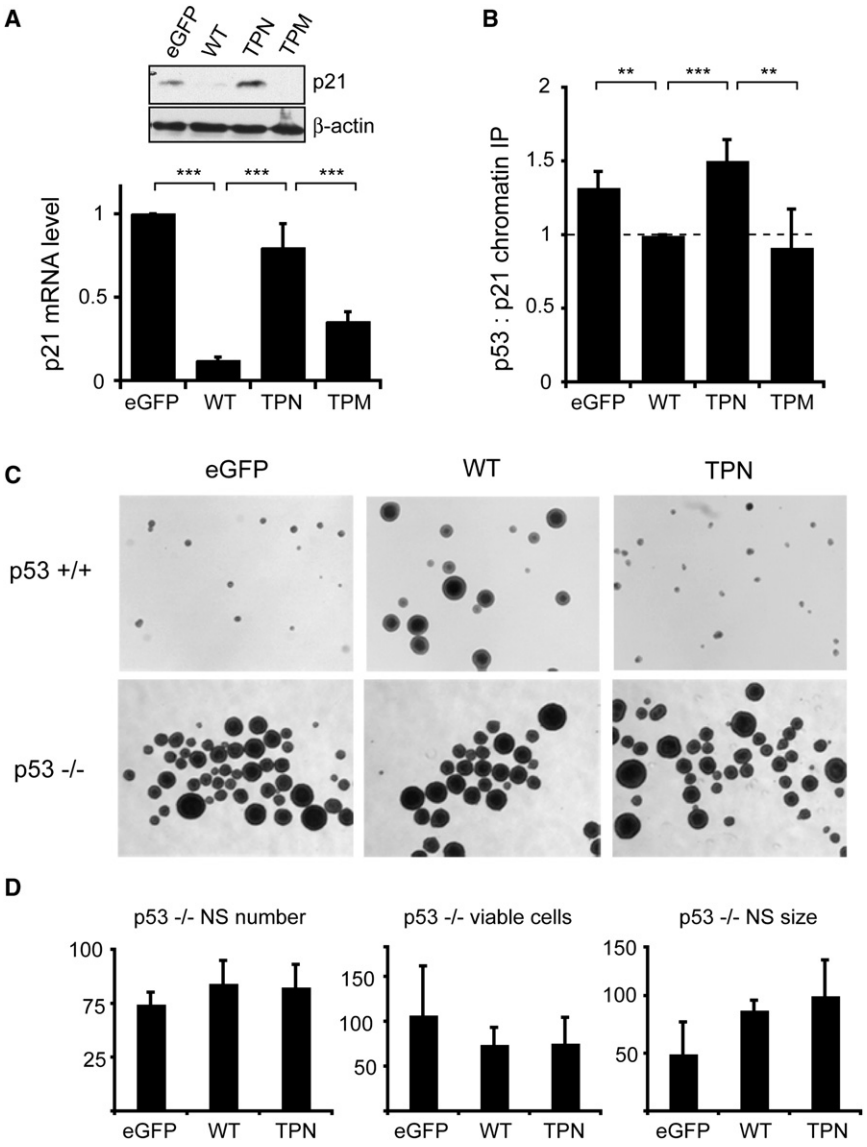

Figure 8. An Oppositional Relationship between Olig2 and p53 in Cycling Neural Progenitors

(A) Endogenous p21 protein (inset) and mRNA (bar graphs) are suppressed by wild-type and phosphomimetic Olig2 in cycling neural progenitors. Olig2$^{-/-}$ mouse neural progenitor cells were stably transduced with vector control (eGFP), WT, TPN, or TPM. Endogenous protein levels were compared by western blotting with p21 antibody and β-actin as control. RNA was extracted from cells as described above, and p21 mRNA levels were quantified using premade p21 TaqMan gene expression assay. Error bars, SD.

(B) Expression of p21 in cycling neural progenitors correlates with p53 loading on promoter/enhancer elements of the p21 promoter. Lysates of Olig2$^{-/-}$ mouse neural progenitor cells stably transduced with vector control (eGFP), WT, TPN, or TPM were processed for ChIP with p53 antibody. Primers spanning the distal E box in the p21 promoter/enhancer region were used for qRT-PCR analysis. Bar graph shows p21 promoter binding normalized for nontarget site enrichment. Note that the differences in p53 loading, between the four groups, though nuanced, are statistically significant (**$p < 0.01$, ***$p < 0.001$) and in good accord with differences noted in acetylated p53 seen in cycling cells (Figure 7B). Error bars, SEM.

(C) Phosphorylation state of Olig2 is irrelevant in p53 null neurospheres. Olig2cre/cre mice were intercrossed to p53fl/fl mice to obtain neural progenitors that were Olig2:p53 double null. These progenitors were transduced with eGFP, wild-type Olig2, or the TPN mutant of Olig2 as indicated. Secondary neurosphere assays were performed on these cells and on matched p53 +/+ controls as per Figure 1.

(D) Quantitation of neurosphere (NS) counts and sizes from (C). Neurosphere size was measured using ImageJ. Error bars, SD.

used have been described previously (Lu et al., 2002; Schuller et al., 2008). Shi mice were obtained from Jackson Laboratory. Neural progenitor cells were isolated from lateral ganglionic eminence (LGE) of E12–E14 embryos from time-pregnant mice using techniques previously described (Qian et al., 1998).

Olig2 Protein Purification and Phosphorylation Analysis

Endogenous Olig2 protein was purified from in vitro-cultured murine LGE neurospheres (5 g total pellet weight; derived from E14 embryos of CD1 time-pregnant mice; Charles River) and human glioma line BT37 mouse xenografts (15 g total tissue weight) by generating nuclear extracts that were then subjected to Olig2 antibody affinity column chromatography. The affinity column was generated using Olig2 antibody according to the instructions of AminoLink Plus Immobilization Kit (Pierce). Purified Olig2 protein was subjected to SDS-PAGE followed by Coomassie blue staining. Bands corresponding to Olig2 protein were excised and sent to the Taplin Biological Mass Spectrometry Facility (Harvard Medical School) for protein identification and Olig2 phosphorylation analysis using LC/MS/MS. Details can be found in Supplemental Experimental Procedures.

Secondary Neurosphere Assay

Olig2-null neural progenitor cell lines were derived from the LGE of individual E14 *Olig2*-null embryos and maintained as neurosphere cultures. After three passages, neurospheres were dissociated into single cells and then transduced with retroviruses containing various mutants of Olig2 at an MOI of 0.5:1 under neurosphere culture conditions. Transduced cells were selected with blasticidin for 7 days. Primary transduced neurospheres were dissociated into single cells and replated at 10 cells/μl in 6-well plates for secondary neurosphere formation assays. For each construct, tertiary neurosphere assays were performed to confirm the results seen in secondary neurosphere assay. The expression of each construct was confirmed with western blot and immunocytochemistry. For total cell population analyses, total neurospheres from each 6-well were collected and mechanically dissociated into single cells. Total viable cells were counted with hemocytometer using 0.2% trypan blue exclusion. Total neurosphere numbers were counted under a dissection microscope. The images of individual neurospheres were taken using a 4× objective, and ImageJ software was used for measuring neurosphere size (area).

Myelination Assay in Shi Mice

Neurospheres isolated from E14.5 Olig2-null embryos were stably transduced with retrovirus expressing eGFP, Olig2-wt-V5, or Olig2-TPN-V5. Transduced neurospheres were dissociated into single-cell suspension, and 50,000–150,000 cells were injected into the lateral ventricles of homozygous newborn Shi mice (Jackson Laboratory). Recipient mice were sacrificed at postnatal day 30, perfused, and postfixed overnight with 4% paraformaldehyde. Brains were dissected, sectioned at 50 μm, and stained for chicken anti-GFP (Aves Labs), rat anti-MBP (Chemicon), and rabbit anti-V5 (Invitrogen).

^{32}P Labeling of Cells

Cells were labeled for 2 hr in phosphate-free media supplemented with 300 μCi/ml ^{32}P orthophosphate. Cells were washed in cold PBS and protein extracts generated using RIPA buffer. Olig2 was immune precipitated using a pan-olig2 antibody (Arnett et al., 2004) and resolved using SDS-PAGE. Quantitation of the signal was performed using a Typhoon Trio (GE Healthcare).

Generation and Characterization of Phospho-Specific Antibodies

Phosphorylation state-specific antibodies were generated and purified as described previously (Alberta and Segal, 2001) using a peptide containing the triple phosphorylation motif (LVSpSRPpSpSPEPDDLC) conjugated to KLH using the Imject Conjugation kit (Pierce) as antigen in rabbits by Covance (Denver, PA, USA).

Limiting Dilution Tumorigenesis Assay

Two *Ink4A*$^{-/-}$*ARF*$^{-/-}$ *Olig2*$^{-/-}$ *EGFRVIII* neurosphere lines (EB5 and EB7) were generated as described (Ligon et al., 2007), and then stably transduced with eGFP, Olig2 WT, and Olig2 mutants of interest via retroviral infection and five passages of neurosphere expansion. For each Olig2 construct, serial dilutions of cells at 1×10^5, 1×10^4, 1×10^3, and 1×10^2 were injected into the right striatum of Icr-SCID mice (Taconic Farms, Inc.) at the coordinates: A, −0.5 mm; L, 1.50 mm; and D, 2.65 mm, relative to the bregma. Animals were sacrificed at the onset of neurological/clinical symptoms.

ChIP

Olig2$^{-/-}$ mouse neural progenitor cells were stably transduced with retrovirus expressing eGFP, Olig2 WT, Olig2 TPN, or Olig2 TPM as described above. Cells were plated at a density of 10 cells/μl and cultured on laminin-coated 6-well plates (Pollard et al., 2009). Cells were crosslinked with 1% formaldehyde for 10 min at RT. Reaction was quenched with 125 mM glycine for 5 min at RT. The cells were washed twice, and harvested in ice-cold PBS, resuspended in 300 μl SDS lysis buffer, and sonicated with three pulses of 10 s each. Chromatin was diluted in ChIP dilution buffer and precleared for 1 hr at 4°C in the presence of 25 μl Dynal magnetic beads (Invitrogen). For immunoprecipitation, 50 μl beads were incubated with p53 antibody (Santa Cruz) for 5 hr at 4°C. Precleared chromatin and antibody-bound beads were incubated overnight on a rotor at 4°C. Beads were then washed six times in RIPA wash buffer and twice in TE. Beads were resuspended in 100 μl buffer (200 mM NaCL, 1% SDS, and 0.1 M NaHCO3) and reverse crosslinked overnight at 65°C. Immunoprecipitated DNA was cleaned with PCR cleanup kit (QIAGEN) and eluted in ddH2O.

Quantitative PCR

Chromatin-immunoprecipitated DNA was analyzed with quantitative PCR in real-time PCR system (Applied Biosystems), using SYBR green mix. Primers used for qPCR are as described in detail elsewhere (Mehta et al., 2011). Presented data are delta CT values normalized for WT promoter occupancy.

Radiation Sensitivity Assay

Olig2$^{-/-}$ mouse neural progenitor cells stably transduced with eGFP, Olig2 WT, Olig2 TPN, or Olig2 TPM were cultured under adherent culture condition as described above. Cells were allowed to recover for 3 hr and then treated with 2 Gy irradiation. Control groups remained untreated. At 4–5 days after treatment, viable cells were counted by trypan blue exclusion. Data are presented as percentage of total viable cell number after treatment relative to untreated controls.

Immunoblotting

Total Olig2 immunoblotting was performed according to standard protocols using either a rabbit polyclonal anti-Olig2 antibody (1:100,000) or a monoclonal mouse anti-Olig2 antibody (1:2,000) (Arnett et al., 2004).

SUPPLEMENTAL INFORMATION

Supplemental Information includes Supplemental Experimental Procedures and eight figures and can be found with this article online at doi:10.1016/j.neuron.2011.02.005.

ACKNOWLEDGMENTS

The authors gratefully acknowledge Dr. Ross Tomaino at the Taplin Biological Mass Spectrometry Facility of Harvard Medical School for helpful suggestions in the proteolytic digestions and mass spectroscopy analysis of Olig2. Excellent technical assistance was provided by Diane Goleblowski, Maria Murray, Jessica Weatherbee, and Gizelle Robinson. Finally, we are grateful to Drs. Qiufu Ma and Rosalind Segal at Dana-Farber for support and helpful suggestions. M.A.P. acknowledges KO8 NS062744 for support. This work was supported by grants from the NINDS (NS040511 and NS057727 to D.H.R. and C.D.S., respectively) and from the Pediatric Low-Grade Astrocytoma Foundation. D.H.R is a Howard Hughes Medical Institute Investigator.

Accepted: December 16, 2010
Published: March 9, 2011

REFERENCES

Alberta, J.A., and Segal, R.A. (2001). Generation and utilization of phosphorylation state-specific antibodies to investigate signaling pathways. Curr. Protoc. Neurosci. *3*, 3.14.

Arnett, H.A., Fancy, S.P., Alberta, J.A., Zhao, C., Plant, S.R., Kaing, S., Raine, C.S., Rowitch, D.H., Franklin, R.J., and Stiles, C.D. (2004). bHLH transcription factor Olig1 is required to repair demyelinated lesions in the CNS. Science *306*, 2111–2115.

Bachoo, R.M., Maher, E.A., Ligon, K.L., Sharpless, N.E., Chan, S.S., You, M.J., Tang, Y., DeFrances, J., Stover, E., Weissleder, R., et al. (2002). Epidermal growth factor receptor and Ink4a/Arf: convergent mechanisms governing terminal differentiation and transformation along the neural stem cell to astrocyte axis. Cancer Cell *1*, 269–277.

Barlev, N.A., Liu, L., Chehab, N.H., Mansfield, K., Harris, K.G., Halazonetis, T.D., and Berger, S.L. (2001). Acetylation of p53 activates transcription through recruitment of coactivators/histone acetyltransferases. Mol. Cell *8*, 1243–1254.

Beatus, P., and Lendahl, U. (1998). Notch and neurogenesis. J. Neurosci. Res. *54*, 125–136.

Cai, J., Chen, Y., Cai, W.H., Hurlock, E.C., Wu, H., Kernie, S.G., Parada, L.F., and Lu, Q.R. (2007). A crucial role for Olig2 in white matter astrocyte development. Development *134*, 1887–1899.

Cancer Genome Atlas Research Network. (2008). Comprehensive genomic characterization defines human glioblastoma genes and core pathways. Nature *455*, 1061–1068.

Coleman, M.L., Marshall, C.J., and Olson, M.F. (2003). Ras promotes p21 (Waf1/Cip1) protein stability via a cyclin D1-imposed block in proteasome-mediated degradation. EMBO J. *22*, 2036–2046.

Dornan, D., Shimizu, H., Perkins, N.D., and Hupp, T.R. (2003). DNA-dependent acetylation of p53 by the transcription coactivator p300. J. Biol. Chem. *278*, 13431–13441.

Edlund, T., and Jessell, T.M. (1999). Progression from extrinsic to intrinsic signaling in cell fate specification: a view from the nervous system. Cell *96*, 211–224.

Gong, J., Ammanamanchi, S., Ko, T.C., and Brattain, M.G. (2003). Transforming growth factor beta 1 increases the stability of p21/WAF1/CIP1

protein and inhibits CDK2 kinase activity in human colon carcinoma FET cells. Cancer Res. *63*, 3340–3346.

Jackson, E.L., Garcia-Verdugo, J.M., Gil-Perotin, S., Roy, M., Quinones-Hinojosa, A., VandenBerg, S., and Alvarez-Buylla, A. (2006). PDGFR alpha-positive B cells are neural stem cells in the adult SVZ that form glioma-like growths in response to increased PDGF signaling. Neuron *51*, 187–199.

Jessell, T.M. (2000). Neuronal specification in the spinal cord: inductive signals and transcriptional codes. Nat. Rev. Genet. *1*, 20–29.

Justice, N.J., and Jan, Y.N. (2002). Variations on the Notch pathway in neural development. Curr. Opin. Neurobiol. *12*, 64–70.

Kageyama, R., and Nakanishi, S. (1997). Helix-loop-helix factors in growth and differentiation of the vertebrate nervous system. Curr. Opin. Genet. Dev. *7*, 659–665.

Kippin, T.E., Martens, D.J., and van der Kooy, D. (2005). p21 loss compromises the relative quiescence of forebrain stem cell proliferation leading to exhaustion of their proliferation capacity. Genes Dev. *19*, 756–767.

Kleihues, P., and Cavenee, W.K. (2007). Tumours of the Central Nervous System, Fourth Edition (Lyon, France: IARC Press).

Lee, J.E. (1997). Basic helix-loop-helix genes in neural development. Curr. Opin. Neurobiol. *7*, 13–20.

Lee, S.K., Lee, B., Ruiz, E.C., and Pfaff, S.L. (2005). Olig2 and Ngn2 function in opposition to modulate gene expression in motor neuron progenitor cells. Genes Dev. *19*, 282–294.

Li, M., Luo, J., Brooks, C.L., and Gu, W. (2002). Acetylation of p53 inhibits its ubiquitination by Mdm2. J. Biol. Chem. *277*, 50607–50611.

Ligon, K.L., Alberta, J.A., Kho, A.T., Weiss, J., Kwaan, M.R., Nutt, C.L., Louis, D.N., Stiles, C.D., and Rowitch, D.H. (2004). The oligodendroglial lineage marker OLIG2 is universally expressed in diffuse gliomas. J. Neuropathol. Exp. Neurol. *63*, 499–509.

Ligon, K.L., Kesari, S., Kitada, M., Sun, T., Arnett, H.A., Alberta, J.A., Anderson, D.J., Stiles, C.D., and Rowitch, D.H. (2006). Development of NG2 neural progenitor cells requires Olig gene function. Proc. Natl. Acad. Sci. USA *103*, 7853–7858.

Ligon, K.L., Huillard, E., Mehta, S., Kesari, S., Liu, H., Alberta, J.A., Bachoo, R.M., Kane, M., Louis, D.N., Depinho, R.A., et al. (2007). Olig2-regulated lineage-restricted pathway controls replication competence in neural stem cells and malignant glioma. Neuron *53*, 503–517.

Lu, Q.R., Yuk, D., Alberta, J.A., Zhu, Z., Pawlitzky, I., Chan, J., McMahon, A.P., Stiles, C.D., and Rowitch, D.H. (2000). Sonic hedgehog–regulated oligodendrocyte lineage genes encoding bHLH proteins in the mammalian central nervous system. Neuron *25*, 317–329.

Lu, Q.R., Sun, T., Zhu, Z., Ma, N., Garcia, M., Stiles, C.D., and Rowitch, D.H. (2002). Common developmental requirement for Olig function indicates a motor neuron/oligodendrocyte connection. Cell *109*, 75–86.

Mehta, S., Huillard, E., Kesari, S., Maire, C.L., Geolebiowski, D., Harrington, E.P., Alberta, J.A., Kane, M.F., Theisen, M., Ligon, K.L., et al. (2011). The CNS-restricted transcription factor Olig2 opposes p53 responses to genotoxic damage in neural progenitors and malignant glioma. Cancer Cell *19*, in press.

Meletis, K., Wirta, V., Hede, S.M., Nister, M., Lundeberg, J., and Frisen, J. (2006). p53 suppresses the self-renewal of adult neural stem cells. Development *133*, 363–369.

Menn, B., Garcia-Verdugo, J.M., Yaschine, C., Gonzalez-Perez, O., Rowitch, D., and Alvarez-Buylla, A. (2006). Origin of oligodendrocytes in the subventricular zone of the adult brain. J. Neurosci. *26*, 7907–7918.

Novitch, B.G., Chen, A.I., and Jessell, T.M. (2001). Coordinate regulation of motor neuron subtype identity and pan-neuronal properties by the bHLH repressor Olig2. Neuron *31*, 773–789.

Park, H.C., Mehta, A., Richardson, J.S., and Appel, B. (2002). olig2 is required for zebrafish primary motor neuron and oligodendrocyte development. Dev. Biol. *248*, 356–368.

Parras, C.M., Galli, R., Britz, O., Soares, S., Galichet, C., Battiste, J., Johnson, J.E., Nakafuku, M., Vescovi, A., and Guillemot, F. (2004). Mash1 specifies neurons and oligodendrocytes in the postnatal brain. EMBO J. *23*, 4495–4505.

Petryniak, M.A., Potter, G.B., Rowitch, D.H., and Rubenstein, J.L. (2007). Dlx1 and Dlx2 control neuronal versus oligodendroglial cell fate acquisition in the developing forebrain. Neuron *55*, 417–433.

Pollard, S.M., Yoshikawa, K., Clarke, I.D., Danovi, D., Stricker, S., Russell, R., Bayani, J., Head, R., Lee, M., Bernstein, M., et al. (2009). Glioma stem cell lines expanded in adherent culture have tumor-specific phenotypes and are suitable for chemical and genetic screens. Cell Stem Cell *4*, 568–580.

Qian, X., Goderie, S.K., Shen, Q., Stern, J.H., and Temple, S. (1998). Intrinsic programs of patterned cell lineages in isolated vertebrate CNS ventricular zone cells. Development *125*, 3143–3152.

Ross, S.E., Greenberg, M.E., and Stiles, C.D. (2003). Basic helix-loop-helix factors in cortical development. Neuron *39*, 13–25.

Rowitch, D.H. (2004). Glial specification in the vertebrate neural tube. Nat. Rev. Neurosci. *5*, 409–419.

Schuller, U., Heine, V.M., Mao, J., Kho, A.T., Dillon, A.K., Han, Y.G., Huillard, E., Sun, T., Ligon, A.H., Qian, Y., et al. (2008). Acquisition of granule neuron precursor identity is a critical determinant of progenitor cell competence to form Shh-induced medulloblastoma. Cancer Cell *14*, 123–134.

Setoguchi, T., and Kondo, T. (2004). Nuclear export of OLIG2 in neural stem cells is essential for ciliary neurotrophic factor-induced astrocyte differentiation. J. Cell Biol. *166*, 963–968.

Sun, T., Dong, H., Wu, L., Kane, M., Rowitch, D.H., and Stiles, C.D. (2003). Cross-repressive interaction of the Olig2 and Nkx2.2 transcription factors in developing neural tube associated with formation of a specific physical complex. J. Neurosci. *23*, 9547–9556.

Takebayashi, H., Yoshida, S., Sugimori, M., Kosako, H., Kominami, R., Nakafuku, M., and Nabeshima, Y. (2000). Dynamic expression of basic helix-loop-helix Olig family members: implication of Olig2 in neuron and oligodendrocyte differentiation and identification of a new member, Olig3. Mech. Dev. *99*, 143–148.

Takebayashi, H., Nabeshima, Y., Yoshida, S., Chisaka, O., Ikenaka, K., and Nabeshima, Y. (2002). The basic helix-loop-helix factor olig2 is essential for the development of motoneuron and oligodendrocyte lineages. Curr. Biol. *12*, 1157–1163.

Zhou, Q., and Anderson, D.J. (2002). The bHLH transcription factors OLIG2 and OLIG1 couple neuronal and glial subtype specification. Cell *109*, 61–73.

Zhou, Q., Wang, S., and Anderson, D.J. (2000). Identification of a novel family of oligodendrocyte lineage-specific basic helix-loop-helix transcription factors. Neuron *25*, 331–343.

Zhou, Q., Choi, G., and Anderson, D.J. (2001). The bHLH transcription factor Olig2 promotes oligodendrocyte differentiation in collaboration with Nkx2.2. Neuron *31*, 791–807.